Gain Roll-off in Cadmium Selenide Colloidal

Quantum Wells under Intense Optical Excitation

Benjamin T. Diroll, 1* Alexandra Brumberg, 2 and Richard D. Schaller 1,2

¹Center for Nanoscale Materials, Argonne National Laboratory, 9700 S. Cass Avenue, Lemont, Illinois 60439, United States

²Department of Chemistry, Northwestern University, 2145 Sheridan Road, Evanston, Illinois 60208, United States

KEYWORDS. Colloidal quantum wells, nanoplatelets, gain, amplified spontaneous emission, lasing

ABSTRACT

Colloidal quantum wells, or nanoplatelets, show among the lowest thresholds for amplified spontaneous emission and lasing among solution-cast materials and among the highest modal gains of any known materials. Using solution measurements of colloidal quantum wells, this work shows that under optical excitation, optical gain increases with pump fluence before rolling off due to broad photoinduced absorption at energies lower than the band gap. Despite the common occurrence of gain induced by an electron-hole plasma found in bulk materials and epitaxial quantum wells, under no measurement conditions was the excitonic absorption of the colloidal

quantum wells extinguished and gain arising from a plasma observed. Instead, like gain, excitonic absorption reaches a minimum intensity near a photoinduced carrier sheet density of 2×10^{13} cm⁻² above which the absorption peak becomes *more* intense. To understand the origins of these saturation and reversal effects, measurements were performed with different excitation wavelengths, which deposit differing amounts of excess energy above the band gap. Across many samples, it was consistently observed that a less energetic excitation results stronger excitonic bleaching and gain for a given carrier density. Transient and static optical measurements at elevated temperatures, as well as transient X-ray diffraction of the samples, suggest that origin of gain saturation and reversal is a heating and disordering of the colloidal quantum wells which produces sub-gap photoinduced absorption.

Cadmium selenide colloidal quantum wells (CQWs), frequently called nanoplatelets, are promising materials for solution-based optical gain media. CQWs exhibit low thresholds for amplified spontaneous emission and lasing spanning visible wavelengths^{1–6} and the largest modal gain of any nanomaterials,⁷ enabling even continuous wave operation.^{3,8} Driven by large exciton binding energies, optical gain and lasing action in CdSe CQWs is reported to occur due to a biexcitonic state, similar to other colloidal quantum dots.^{3,9} This is distinct from most epitaxial quantum wells in which gain, particularly near ambient temperatures, is most commonly observed from free electron-hole plasmas. This work explores the possibility of generating a carrier plasma in CdSe CQWs under intense optical excitation via the Mott transition, in which the density of excitation destabilizes excitons, yielding a carrier plasma. Mott transitions from biexcitonic gain to plasma gain have been observed in related epitaxial quantum wells¹⁰ and nanowires.¹¹ Previous works have speculated that gain in CQWs may saturate due to a phase space filling with excitons

or a Mott transition at high excitation intensities (>1 mJ·cm⁻²)⁷ One literature report indicates the coexistence of both excitonic absorption and electron-hole plasma.¹²

By examining the extinction of the CQWs at such high fluences in several samples with different thicknesses, however, we do not observe a plasma. Rather, similar to quantum dots, 13 under increasingly intense optical excitation, biexcitonic gain saturates, diminishes, and even reverts to loss due to the formation of a broadband photoinduced absorption at energies below the band gap. Under the same photoexcitation conditions, the excitonic absorption bleaches up to electron-hole sheet densities of c. 2×10^{13} cm⁻² above which more intense excitation results in *increasing* excitonic absorption. A similar phenomenon is observed in all measured samples, including core/shell CQWs. In epitaxial quantum wells, gain saturation may be related to phase space filling of excitons 14 or formation of electron-hole plasmas. 15 In this case, however, several lines of evidence indicate a thermal origin of the saturation and reversal of gain at high excitation intensities, including experiments using different photon energies of the excitation, static thermal difference measurements, and transient X-ray diffraction.

Results and Discussion

Light Amplification in Colloidal Quantum Wells. Figure 1 shows typical absorption, transmission, electron microscopy, and optical spectroscopy of CdSe CQWs. In Figure 1a shows the linear absorption dipole (μ) of 4.5 monolayer (ML, 4 monolayers of Se and 5 monolayers of Cd) and 5.5 ML samples based upon literature reports. ¹⁶ The monolayer thickness defines the position of the strong excitonic transitions, which belong to heavy-hole (HH), light-hole (LH), and split-off bands. ¹⁷ Atomic precision in thickness across the sample, despite polydisperse lateral dimensions as shown in Figure 1b, yields narrow optical transitions in absorption and emission.

Figure S1 contains transmission electron microscope images of other samples featured in this work. Fluence dependent emission of dilute solutions of CdSe CQWs (Figure 1c) shows a pronounced broadening and increased emission at lower energies attributed to biexcitonic emission.³ In a dense film as in Figure 1d, above threshold fluences, an amplified spontaneous emission (ASE) feature also emerges at energies ~50 meV lower than the photoluminescence peak under weak excitation.

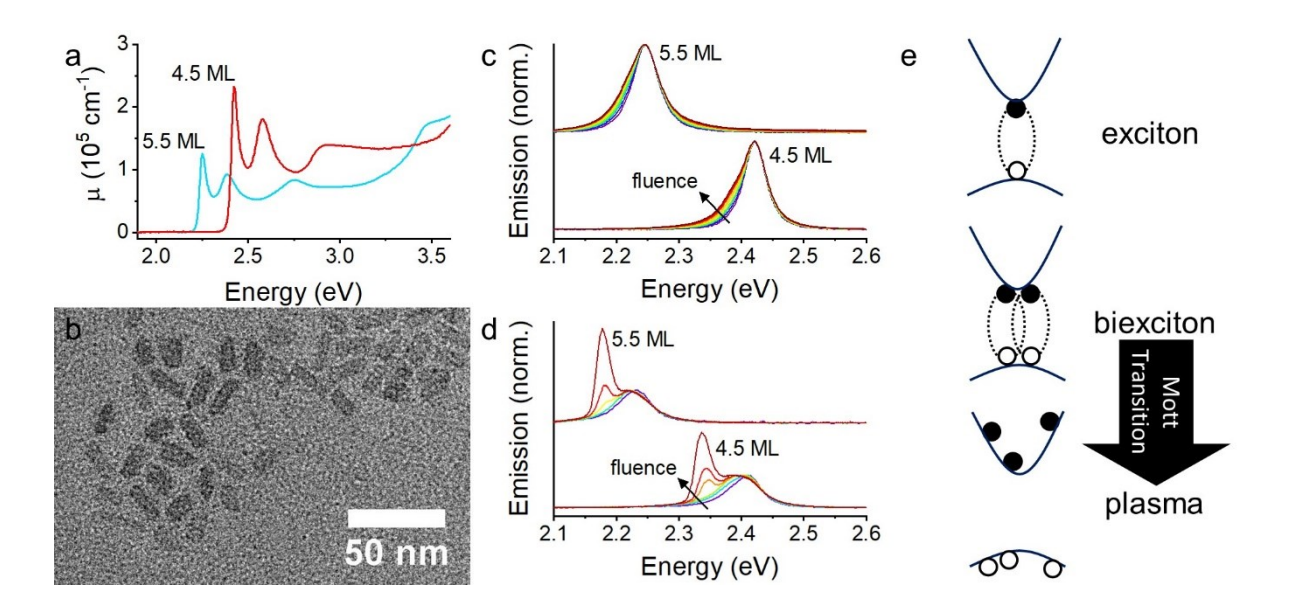


Figure 1. (a) Absorption dipoles of 4.5 and 5.5 monolayer (ML) CdSe colloidal quantum wells (CQWs). (b) Typical TEM image of 4.5 ML CdSe CQW sample. (c) Normalized, fluence-dependent emission of CQW solutions. (d) Normalized, fluence-dependent emission of CQW films illuminated with 400 μ m diameter spot. Normalization is to the excitonic emission peak. (e) Cartoon of single exciton, biexciton, and transition to unbound carrier plasma.

The origin of ASE in CdSe CQWs has been intensively studied. Underpinning the reported physics of CQW lasing is that they have exciton binding energies far greater than thermal energy at 300 K. Reported exciton binding energies for 4.5 ML and 5.5 ML CQWs are 160-200 meV, ^{18–20} which is sufficiently large that excitons are anticipated to dominate the physics of these samples up to the melting point. ²¹ As a consequence, gain and lasing in CQWs is observed from biexcitonic species (at times termed "excitonic molecules"), as shown in the cartoon in Figure 1e. ^{1,3,22} The

exact number of excitons per particle corresponding to the transparency condition $(A + \Delta A = 0)$ and enabling gain depends on the lateral area of the CQWs, but corresponds to an electron-hole density of c. 2.5×10¹² cm⁻² in 4.5 ML CQWs.²² All previous reports of ASE or lasing have been consistent with this biexcitonic mechanism. This is distinct from epitaxial quantum wells in which biexciton lasing may be observed at low temperatures in some samples, but plasma type lasing is ordinarily found at higher temperatures at which thermal energy is greater than the exciton binding energy. 23-25 In principle, gain from a plasma can also be observed at the Mott transition at which electron-hole densities reach a level that the available space per exciton is comparable to the Bohr radius. 15 Such high excitation densities destabilize excitons and result in an electron-hole plasma. Mott transitions have been observed in bulk and quantum forms of GaAs, 11,26,27 ZnO, 28,29 CdS, 28 and InGaAs quantum wells, 10 and, despite very large exciton binding energies, in transition metal dichalcogenides. ³⁰ The formation of an electron-hole plasma extinguishes excitonic absorption and is accompanied by a blue-shift of photoluminescence intensity and absorption associated with the continuous density of states of free carriers. 10,14,26 However, there is no unambiguous evidence from photoemission experiments or gain spectroscopy that full Mott transitions occur—and, if so, at what densities—in CQWs. Only one report, based upon transient absorption spectroscopy, indicates the formation of a plasma which nonetheless coexists with biexcitonic gain, an apparent contradiction.¹²

Gain spectroscopy of Colloidal Quantum Wells. To examine the formation of an electron-hole plasma in CdSe CQWs, transient absorption was performed on several 4.5 ML and 5.5 ML samples at variable excitation fluence. To ensure, as best as possible, that the results do not reflect photocharging or irreversible sample changes, samples were vigorously stirred during measurements and data presented in this work represents reproducible transient spectra of multiple

runs of the optical delay track. The results of these experiments, with transient spectra collected at 3 ps pump-probe delay, which allows relaxation of photoexcited carriers, are shown in normalized plots in Figures 2a and 2b. Raw ΔA data is presented in Figure S2. Several phenomena occur in both fluence-dependent series: (i) initially narrow bleaching features broaden substantially at carrier density up to c. 2×10¹³ cm⁻²; (ii) the bleaching intensity of the light-hole feature continuously increases relative to the heavy-hole band edge bleach with increasing fluence; and (iii) at the electron-hole densities greater than 2×10¹³ cm⁻², a broad photoinduced absorption appears at energies below the excitonic absorption. The photoinduced absorption or gain, generated using $A+\Delta A$, for the two samples are shown in Figures 2c and 2d, respectively, with an expansion of the region showing gain shown in Figures 2e and 2f. Although not apparent in the normalized datasets but shown in Figures 2c and 2d (and Figure S2), the excitonic bleach feature of the CQWs first decreases, due to bleaching, but this effect saturates and then reverses. A related effect is apparent in the gain. Earlier reports of the gain spectrum of CdSe CQWs show very similar gain spectra up to electron-hole densities of c. 1×10^{13} cm⁻² and lower, 1,12,22,31,32 which corresponds roughly, depending on the CQW size and excitation photon energy, with fluences $>500 \, \mu J \cdot cm^{-2}$ or exciton numbers >30 per CQW. Most earlier literature does not report results for higher excitation densities, but in one report from Tomar et al., 12 a second band of gain is observed at 2.45 eV for 4.5 ML samples. This was not observed in here for any of several samples, including (as shown in Figure S3) core/shells: at the highest carrier densities, the photoinduced absorption results in substantially diminished gain bandwidth, similar to observed photoinduced absorptions in CdSe quantum dots, ¹³ and no second band of gain is observed.

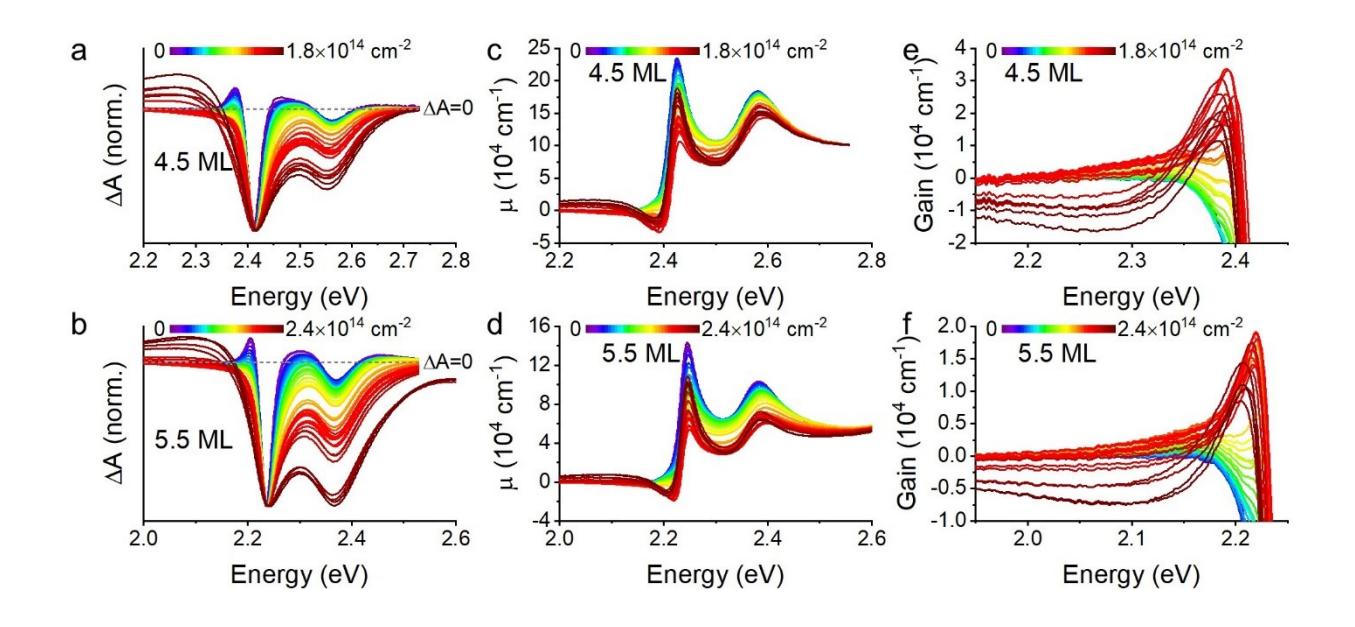


Figure 2 (a, b) Normalized transient absorption spectra (ΔA) of a representative (a) 4.5 and (b) 5.5 ML CQW samples as a function of photogenerated sheet density. Each spectrum is collected at a 3 ps pump-probe delay for many powers of 3.5 eV pump light. (c, d) Absorption dipole calculated for many photogenerated sheet densities of the same (c) 4.5 and (d) 5.5 ML samples. (e, d) Zoomed in regions of (c) and (d), respectively, showing the spectral window of gain.

The trends apparent in Figure 2 are quantified in Figures 3 and 4 across three samples each of 4.5 ML and 5.5 ML thicknesses using two excitation photon energies, 3.50 eV and 2.72 eV (see Figure S4). Here, data are presented as a function of the electron-hole density of the samples, rather than fluence, which does not account for energy differences of the pump excitations, or exciton number, which does not account for differences in the CQW physical dimensions. Other representations may be found in Figure S5. Individual points show the data for different CQW samples and the solid and dashed lines show the smoothed averaged data of all the samples with either 3.50 eV (solid) or 2.72 eV (dashed) pump photon energy. Figures 3a and 3b show the normalized intensity of the first excitonic absorption associated with the heavy hole of 4.5 ML and 5.5 ML CQWs, respectively, as a function of the electron-hole density of the samples. Bleaching of the exciton was consistently greater under photoexcitation with 2.72 eV photons, compared to 3.50 eV photoexcitation, but in both cases, the bleaching saturates and reverses for electron-hole

excitation densities greater than 2×10¹³ cm⁻². It is noted that a related phenomenon has been observed in core/shell CQW systems in saturable absorption experiments, attributed to potential exciton-exciton interactions or enhanced upconversion of higher-energy LH excitons from HH excitons.³³ This second explanation is consistent with data in Figures 3c and 3d, showing larger LH to HH ratios.

The ratio of LH to HH bleaching intensity is a function of carrier density via state filling and temperature (*vida infra*). As shown in Figures 3c and 3d, the ratio of the LH bleaching intensity is consistently larger, for similar initial carrier density, for the 2.72 eV pump than the 3.50 eV pump. The stronger intensity of excitonic bleaching of *both* HH and LH transitions under 2.72 eV photon energy excitation may be explained by higher effective quantum yield with less energetic photons, although reports of the energy-dependent quantum yield are contested.^{34–37} A second effect accompanying more intense photoexcitation is captured in Figures 3e and 3f, showing the half-width at half-maximum of the transient absorption heavy hole bleach features. The broadening of the transient absorption bleaching features at high electron-hole densities, which appears largely insensitive to the photoexcitation energy, reflects both multiple exciton physics (*e.g.* the formation of biexcitonic species) and increases in lattice temperature, as demonstrated in temperature-dependent spectroscopy below.

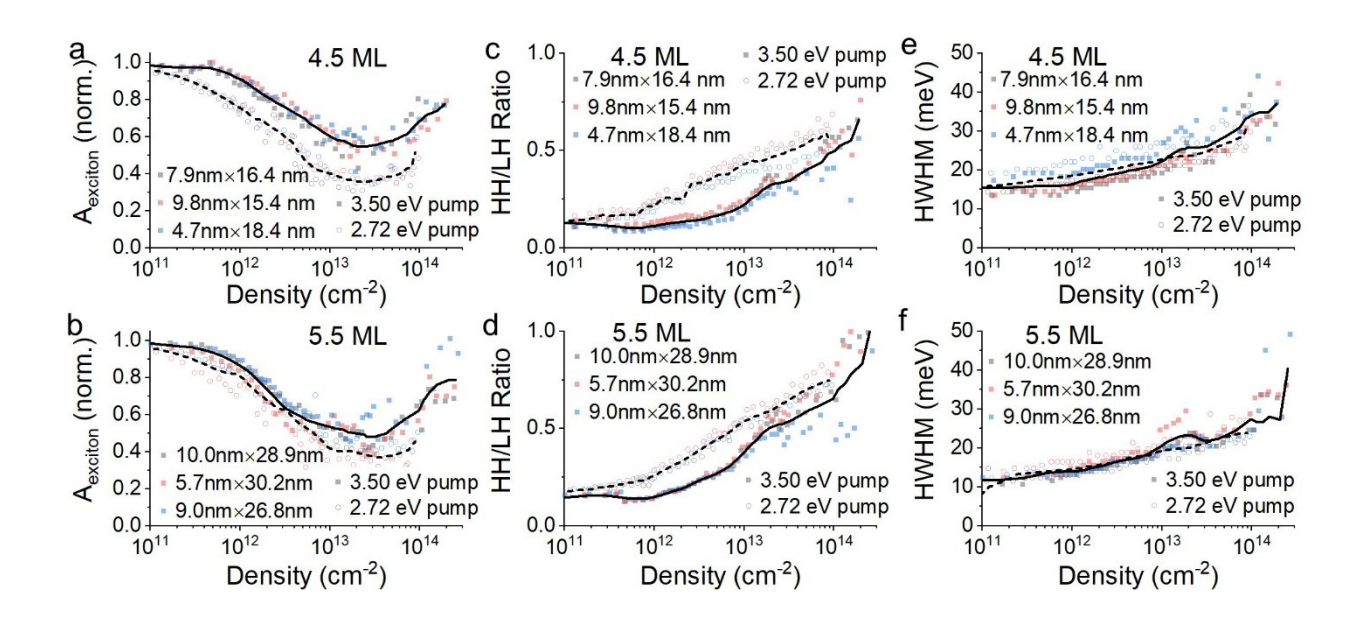


Figure 3. (a, b) Normalized exciton absorption intensity at a pump-probe delay of 3 ps for three (a) 4.5 and (b) 5.5 ML CQW samples as a function of photogenerated sheet density. Each spectrum is collected at a 3 ps pump-probe delay for many powers of 3.5 eV pump light. (c, d) Ratio of heavy hole and light hole bleach signals as a function of photogenerated sheet densities for the same (c) 4.5 and (d) 5.5 ML samples. (e, f) Half-width at half-maximum (HWHM) of the HH bleach feature from the transient absorption spectrum (ΔA) plotted against photogenerated sheet densities of the same (e) 4.5 and (f) 5.5 ML samples. In all cases, data for measurements with 3.5 eV pump are shown in solid symbols and data for 2.72 eV pump measurements are shown in open symbols. A solid line represents a smoothed average of 3.5 eV pump experiments and a dashed line corresponds to the smoothed average of 2.72 eV pump.

The observable gain in CQWs under the same photoexcitation conditions is analyzed at a few representative energies for the 4.5 ML and 5.5 ML samples in Figure 4. Similar to earlier work, ²² peak gain values, achieved at the highest energies monitored in Figure 4, reach values of 20000-30000 cm⁻¹, which is at least qualitatively consistent with the large gain coefficients observed in variable stripe measurements. ⁷ In all observed cases, similar to the persistent excitonic absorption, a blueshift and broadening of gain associated with a Mott transition is not observed. Instead, at excitation intensities greater than 2×10¹³ cm⁻², modal gain saturates and reverses at all measured wavelengths and is not observed at all for energies larger than the HH excitonic transition. Gain is consistently greater and saturates at slightly higher electron-hole densities using 2.72 eV photoexcitation as compared to 3.5 eV pumping. This effect is stronger in the case of 4.5

ML CQWs, for which the relative difference in excess energy of the pump excitation above the band gap is much larger.

The absence of the spectral signatures of a Mott transition in CQWs under intense excitation is surprising. CdSe colloidal quantum dots show substantial quenching of the first (1S) excitonic absorption^{13,38,39} as do related transition metal dichalcogenides.³⁰ At electron-hole densities greater than 1×10^{13} cm⁻², the effective radius of carriers is less than one-half of the bulk CdSe Bohr radius (5.6 nm). 40 One explanation is that the in-plane exciton size in CdSe CQWs is much smaller than the Bohr radius of bulk CdSe, comparable to the COW thickness, ^{18,41} or less than one-fifth of the Bohr radius in these samples. Nonetheless, at still higher excitation intensity, a Mott transition remains possible and at the highest excitation intensities used in this work, the effective radius available per exciton is <1 nm. Instead, as apparent in the absorption and gain spectra of Figure 2, photoinduced absorption is the origin of the gain reversal at all energies and a narrowing of gain bandwidth. At lower energies such as 2.25 eV for 4.5 ML CQWs or 2.10 eV for 5.5 ML CQWs, the photoinduced absorption yields particularly large losses greater than 10000 cm⁻¹. Such broad, "parasitic" photoinduced absorption was previously observed in CdSe colloidal quantum dot samples. 13 Based upon size-dependent behavior and environmental sensitivity, this phenomenon was attributed to extrinsic electronic states such as traps or interface transitions rather than a thermal origin.

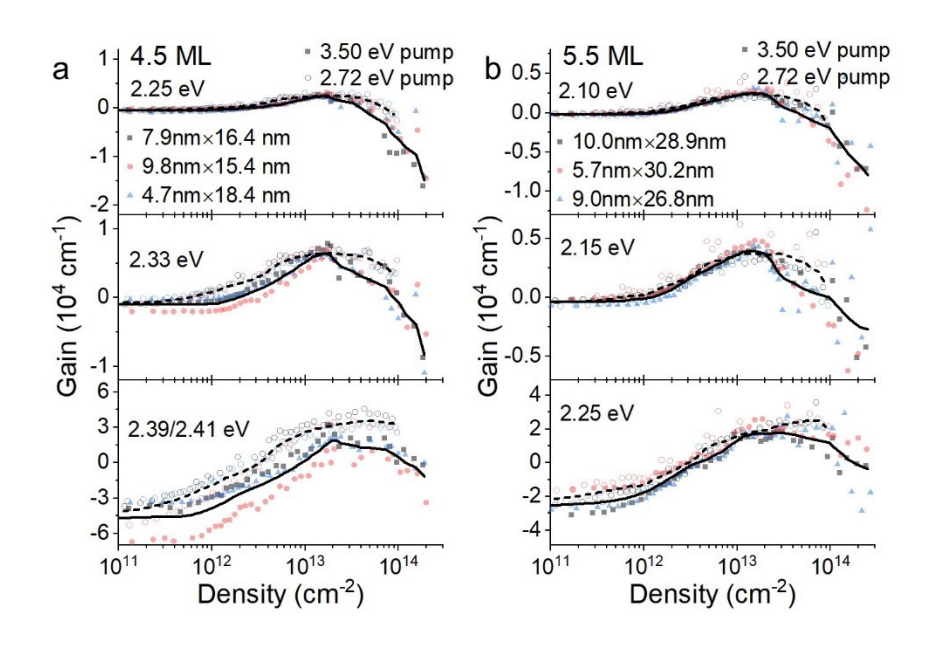


Figure 4. (a, b) Line-cuts of gain or loss at 3 ps pump-probe delay for representative energy values as a function of photogenerated sheet density for (a) 4.5 ML and (b) 5.5 ML CQW samples. In all cases, data for measurements with 3.5 eV pump are shown in solid symbols and data for 2.72 eV measurements are shown in open symbols. A solid line represents a smoothed average of 3.5 eV pump experiments and a dashed line corresponds to the smoothed average of 2.72 eV pump.

Thermal Response Under Intense Photoexcitation. Turning to the origin of the gain saturation and roll off at high excitation fluences, a similar phenomenon observed in colloidal quantum dots centered on the potential role of thermal or electronic effects. ¹³ In that work, Malko *et al.*, showed that cross section of the photoinduced loss was fixed for all quantum dot sizes, completely suppressing gain in small quantum dots, but not in large quantum dots. Based upon sensitivity of the gain to solvent environment (or solid *versus* solution conditions), the photoinduced absorption which parasitized optical gain was attributed to extrinsic electronic effects on the quantum dots, such as interfacial trap sites. Arguing against a thermal origin of gain reversal in CdSe quantum dots, Malko *et al.* reported no red-shifts of the photoluminescence at high intensities which would be associated with the Varshni-like behavior of the CdSe band gap. ¹³

Although the phenomenon observed optically appears to be quite similar in CdSe CQWs and quantum dots, the details are distinct in many respects. In the case of CQWs, several lines of

evidence implicate a thermal origin to the reduction of gain at high excitation intensities. A simple calculation based upon the heat capacity of CdSe, assuming no heat dissipation into the environment, and the excitation densities used in the experiments presented here indicates that the temperature of the CdSe lattice can increase by 100 K or more for electron-hole densities greater than 1×10^{14} cm⁻², with more heating is anticipated for a larger excess photon energy of the pump. (See Supporting Information Figure S6.) For reference, pulsed excitation fluences 3-4 times greater than those used in this work (13-17 mJ·cm⁻²) are reported to reversibly melt bulk CdSe, 42 which has a substantially higher melting point. ^{21,43} The rate of heat dissipation to the environment is therefore critical. Heat outflow from CQWs to methylcyclohexane, which is used for the gain spectroscopy experiments, occurs, at least for small temperature differentials, on a time-scale of c. 160 ps for a 4.5 ML CdSe CQW sample⁴⁴ and c. 240 ps (Figure S7) for the 5.5 ML CdSe CQW sample used in this work. At large temperature differentials, such as those in transient X-ray diffraction, heat loss to a solution environment is on time-scale of hundreds of picoseconds. 45 Dissipation of heat in the solid state is even slower. 44,46,47 Buildup of gain occurs or ASE occurs with intraband relaxation in ~1 ps, based upon time-resolved studies of gain in Figures S8 and S9 and literature data.^{2,12,22} Because the time-scale of heat dissipation is much slower than the buildup of gain, lattice heating of the CQW must necessarily occur of simultaneously with gain and ASE. At the same time heating of the CQWs may have a relatively small influence on time-integrated emission occurring over several nanoseconds, particularly in solutions. The data presented for 2.72 eV and 3.50 eV photon pump energy are at least indicative of the influence of heating arising from the larger excess energy of the 3.50 eV pump. The gain and excitonic bleaching with 2.72 eV photon energy are stronger and do not reverse as substantially, for a given electron-hole density, compared to the 3.50 eV pump.

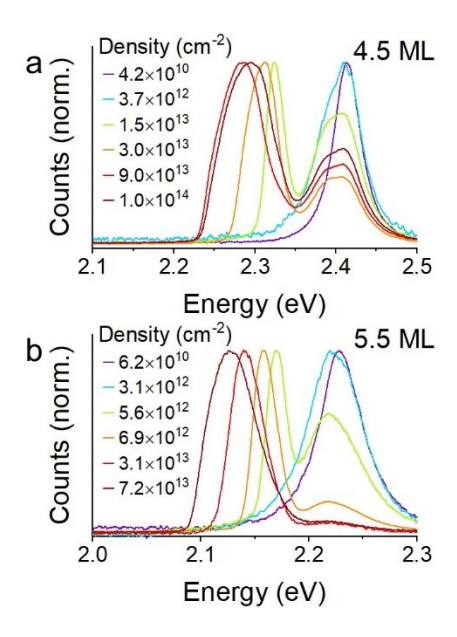


Figure 5. (a, b) High-fluence photoemission from a circular spot of (a) 4.5 ML and (b) 5.5 ML CdSe COWs.

Distinct from earlier reports on quantum dots, the photoluminescence and ASE band of CQWs red-shifts appreciably at electron-hole densities greater than 2×10¹³ cm^{-2,7,12,22} This was further confirmed on exactly the same samples used in Figures 1-4. In these measurements, collection was performed in a front face reflection geometry on semitransparent thin films of 4.5 ML and 5.5 ML CQW samples and a small excitation spot was used to suppress the intensity of ASE and avoid inner filtering effects on the emission. Figure 5 shows the results of high-intensity photoexcitation of CdSe CQW films, in which the band of ASE red-shifts to lower energy at with progressively higher fluence. From Figures 2 and 4, this red-shift is not well-explained by a red-shift in the gain spectrum. Indeed, in the case of 4.5 ML CQWs, the gain band begins to blue-shift as the available gain bandwidth decreases (Figure 5a). Also noteworthy, the relative intensity of the ASE band compared to the excitonic and biexcitonic emission saturates at electron-hole densities of >5×10¹³ cm⁻² for the 5.5 ML sample and for the 4.5 ML sample, the relative intensity of ASE even decreases. This saturation and reduction of ASE intensity is consistent with the

reduction of optical gain at higher electron-hole densities observed by gain spectroscopy on solutions.

Complementing this, static absorption spectra of the 4.5 ML and 5.5 ML CQW samples were also collected (raw data in Figure S10) and the thermal difference spectra (A_T-A_{295 K}) are shown in Figures 6a and 6b overlapped with a transient absorption spectrum collected at high fluence. As anticipated from the thermochromic behavior of CdSe,²¹ increases in the static temperature of the CQWs leads to an increase in the absorption of the film at energies below the band gap, qualitatively resembling the photoinduced absorption feature observed in transient spectroscopy. Both static and low-fluence (<1×10¹² cm⁻²) transient absorption spectra (Figures 6c and 6d) collected at elevated sample temperatures show increases in the LH:HH ratio and the bandwidth of the photoinduced bleach which are catalogued in Figures 6e and 6f, respectively. In particular, the band-width of the transient bleach feature under low fluence at 500 K reaches 25-30 meV, close to the same values reached for photoexcited samples at room temperature with electron-hole densities greater than 1×10¹⁴ cm⁻².

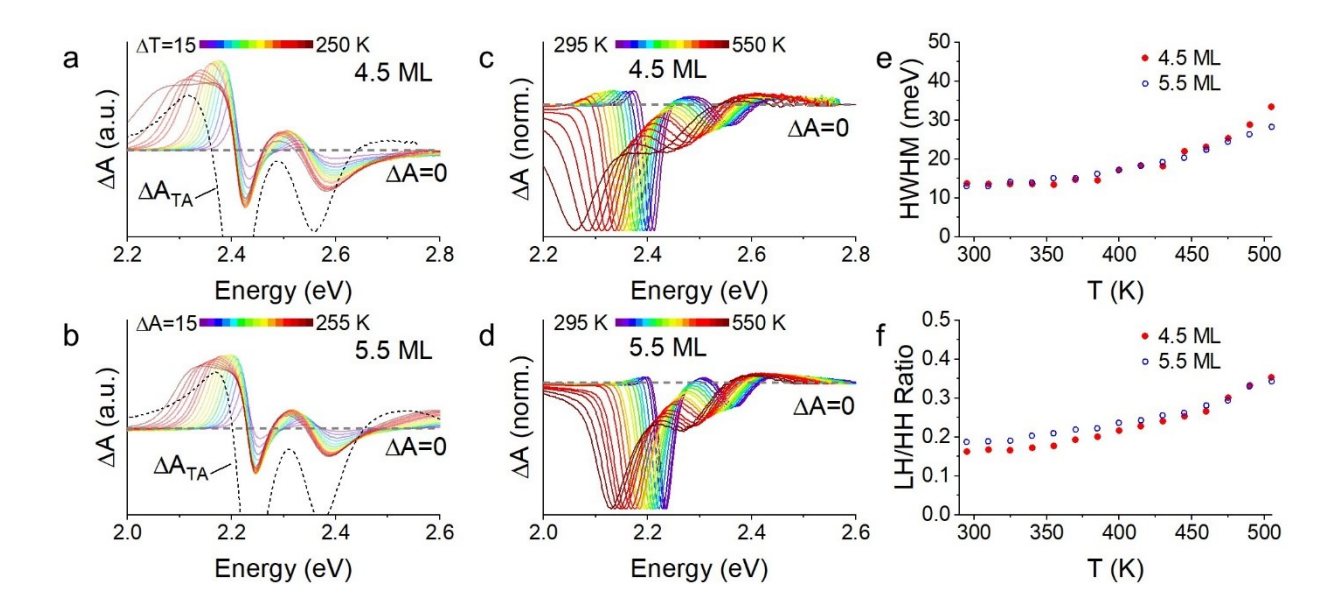


Figure 6. (a, b) Thermal differential absorption spectra ($\Delta A = A_T - A_{295 \text{ K}}$) of (a) 4.5 ML and (b) 5.5 ML CdSe CQWs are shown in colors. The black dashed line shows the ΔA of the same 4.5 or 5.5 ML CdSe CQWs under intense photoexcitation (>5×10¹³ cm⁻²). The plots are scaled for presentation. (c, d) Transient absorption spectra collected at a pump-probe delay of 3 ps and average excitation density $<1\times10^{12}$ cm⁻² as a function of sample temperature. (e) Half-width at half-maximum of transient absorption bleach features as a function of temperature based upon data in figure panels (c) and (d). (f) Ratio of the light hole (LH) and heavy-hole (HH) bleach feature as a function of sample temperature using data in (c) and (d).

Finally, we highlight that there is strong evidence from dynamic measurements of crystallographic structure that CQWs undergo substantial heating and disordering under photoexcitation. Transient X-ray diffraction patterns of 4.5 ML and 5.5 ML CdSe CQWs are shown in Figures 7a and 7b. These data convey the change in X-ray diffraction scattering, Δ S versus q, 40 ps after photoexcitation with 3.10 eV photons overlaid on the static, room temperature diffraction pattern of the sample. As detailed elsewhere, the time-resolved Δ S signal can be broken into two contributions from thermal shifts—which results in close to symmetrical derivative-like Δ S contributions—and disorder or phase transitions, which result in changes in the intensity of diffraction peaks. Although previous work has highlighted that disordering occurs preferentially in the short axis of the CQWs, Figures 7c and 7d show a simplified integration of Δ S signal attributable to disorder and thermal shift by summing contributions of all available

diffraction peaks. The transient X-ray diffraction data shows that at comparable electron-hole excitation densities to the emergence of photoinduced absorption in optical experiments, CQWs show both pronounced heating and disordering of the CQWs. Also, limited temporal dynamics of the transient X-ray diffraction signal (shown in Figure S13) closely matches the dynamics of photoinduced absorption in the same 5.5 ML sample at similar electron-hole densities. As noted above, heating may produce a predictable bathochromic shift of the CQW band gap. The optical properties of CQWs in a molten or substantially disordered state have not been measured experimentally, but calculations of the disordered density of states of CdSe nanoparticles also show pronounced reductions of the band gap. The transient X-ray diffraction data is broadly consisted with attributing the parasitic photoinduced absorption to a photoinduced heating of the CQW lattice.

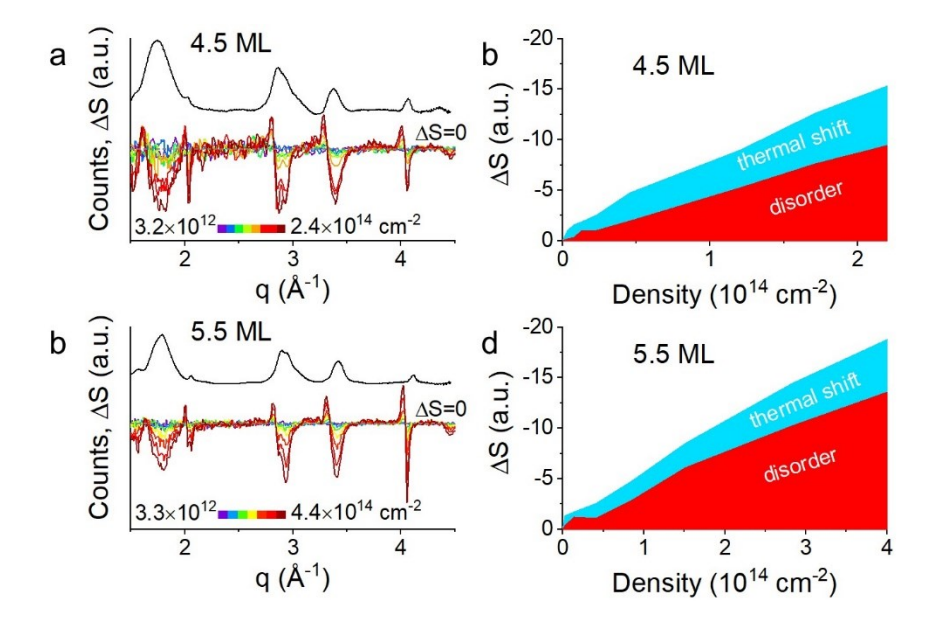


Figure 7. (a, b) Static X-ray diffraction pattern (black line) and transient X-ray diffraction patterns (ΔS) as a function of power at 40 ps pump-probe delay using 3.1 eV pump photon energy. Data are shown for (a) 4.5 ML and (b) 5.5 ML CdSe CQW samples. (c, d) Quantification of the magnitude of ΔS signal as a function of excitation density for the same samples. Total ΔS signal is disambiguated into signal arising from thermal disordering and shift of the diffraction angle.

Conclusions

Collectively, the data presented in this work do not show any indication that the CQWs undergo

an electronic transition from an exciton gas to an electron-hole plasma. These data suggest that

any Mott transition in CdSe CQWs under optical excitation is stillborn, as photoinduced heating

at such intensities alters the structure and optoelectronic properties of the CQW. Lattice heating

results in saturated gain and, at still higher excitation densities, large optical losses due to

photoinduced absorption of hot CQWs. Although resonant excitation at the HH transition is most

likely to generate a Mott transition, due to the minimized energy in excess of the band gap, it

remains unlikely that without modification of the thermal interfaces of the CQW system that such

an optical excitation scheme can generate a Mott transition due to lattice heating arising from

Auger processes. 51,52 This does not preclude the possibility of generating a unipolar plasma, which

is potentially more promising. These results also emphasize the important role that heat dissipation

can play in the performance of nanocrystal-based optoelectronics. Enhancements of the thermal

outflow from CQWs to the environment should allow the realization of even higher levels of gain

saturation.

ASSOCIATED CONTENT

Supporting Information. Experimental details, including synthesis and optical methods, and

additional data may be found in the Supporting Information file.

The following files are available free of charge.

Supporting Information.pdf

AUTHOR INFORMATION

Corresponding Author

17

*bdiroll@anl.gov

Notes

The author declares no conflict of interest.

ACKNOWLEDGMENT

This work was performed at the Center for Nanoscale Materials, a U.S. Department of Energy Office of Science User Facility, and supported by the U.S. Department of Energy, Office of Science, under Contract No. DE-AC02-06CH11357. This research used resources of the Advanced Photon Source, a U.S. Department of Energy (DOE) Office of Science User Facilities operated by Argonne National Laboratory under Contract No. DE-AC02-06CH11357. This material is based upon work supported by the National Science Foundation Graduate Research Fellowship Program under Grant No. DGE-1842165. A.B. gratefully acknowledges support from a 3M Graduate Research Fellowship, the Ryan Fellowship, and the International Institute for Nanotechnology at Northwestern University.

REFERENCES

- She, C.; Fedin, I.; Dolzhnikov, D. S.; Demortière, A.; Schaller, R. D.; Pelton, M.; Talapin,
 D. V. Low-Threshold Stimulated Emission Using Colloidal Quantum Wells. *Nano Lett.*2014, 14 (5), 2772–2777. https://doi.org/10.1021/nl500775p.
- (2) She, C.; Fedin, I.; Dolzhnikov, D. S.; Dahlberg, P. D.; Engel, G. S.; Schaller, R. D.; Talapin, D. V. Red, Yellow, Green, and Blue Amplified Spontaneous Emission and Lasing Using Colloidal CdSe Nanoplatelets. ACS Nano 2015, 9 (10), 9475–9485. https://doi.org/10.1021/acsnano.5b02509.
- (3) Grim, J. Q.; Christodoulou, S.; Di Stasio, F.; Krahne, R.; Cingolani, R.; Manna, L.; Moreels,I. Continuous-Wave Biexciton Lasing at Room Temperature Using Solution-Processed

- Quantum Wells. *Nat. Nanotechnol.* **2014**, *9* (11), 891–895. https://doi.org/10.1038/nnano.2014.213.
- (4) Guzelturk, B.; Kelestemur, Y.; Olutas, M.; Delikanli, S.; Demir, H. V. Amplified Spontaneous Emission and Lasing in Colloidal Nanoplatelets. *ACS Nano* **2014**, *8* (7), 6599–6605. https://doi.org/10.1021/nn5022296.
- (5) Guzelturk, B.; Kelestemur, Y.; Olutas, M.; Li, Q.; Lian, T.; Demir, H. V. High-Efficiency Optical Gain in Type-II Semiconductor Nanocrystals of Alloyed Colloidal Quantum Wells. *J. Phys. Chem. Lett.* 2017, 8 (21), 5317–5324. https://doi.org/10.1021/acs.jpclett.7b02367.
- (6) Diroll, B. T.; Talapin, D. V.; Schaller, R. D. Violet-to-Blue Gain and Lasing from Colloidal CdS Nanoplatelets: Low-Threshold Stimulated Emission Despite Low Photoluminescence Quantum Yield. ACS Photonics 2017, 4 (3), 576–583. https://doi.org/10.1021/acsphotonics.6b00890.
- (7) Guzelturk, B.; Pelton, M.; Olutas, M.; Demir, H. V. Giant Modal Gain Coefficients in Colloidal II-VI Nanoplatelets. *Nano Lett.* **2019**, *19* (1), 277–282. https://doi.org/10.1021/acs.nanolett.8b03891.
- (8) Yang, Z.; Pelton, M.; Fedin, I.; Talapin, D. V.; Waks, E. A Room Temperature Continuous-Wave Nanolaser Using Colloidal Quantum Wells. *Nat. Commun.* 2017, 8 (1), 143. https://doi.org/10.1038/s41467-017-00198-z.
- (9) Park, Y. S.; Roh, J.; Diroll, B. T.; Schaller, R. D.; Klimov, V. I. Colloidal Quantum Dot Lasers. *Nat. Rev. Mater.* 2021, 6 (5), 382–401. https://doi.org/10.1038/s41578-020-00274-9.
- (10) Kappei, L.; Szczytko, J.; Morier-Genoud, F.; Deveaud, B. Direct Observation of the Mott Transition in an Optically Excited Semiconductor Quantum Well. *Phys. Rev. Lett.* 2005, 94

- (14), 1–4. https://doi.org/10.1103/PhysRevLett.94.147403.
- (11) Hayamizu, Y.; Yoshita, M.; Takahashi, Y.; Akiyama, H.; Ning, C. Z.; Pfeiffer, L. N.; West, K. W. Biexciton Gain and the Mott Transition in GaAs Quantum Wires. *Phys. Rev. Lett.*2007, 99 (16), 1–4. https://doi.org/10.1103/PhysRevLett.99.167403.
- (12) Tomar, R.; Kulkarni, A.; Chen, K.; Singh, S.; Van Thourhout, D.; Hodgkiss, J. M.; Siebbeles, L. D. A.; Hens, Z.; Geiregat, P. Charge Carrier Cooling Bottleneck Opens Up Nonexcitonic Gain Mechanisms in Colloidal CdSe Quantum Wells. *J. Phys. Chem. C* 2019, 123 (14), 9640–9650. https://doi.org/10.1021/acs.jpcc.9b02085.
- (13) Malko, A. V.; Mikhailovsky, A. A.; Petruska, M. A.; Hollingsworth, J. A.; Klimov, V. I. Interplay between Optical Gain and Photoinduced Absorption in CdSe Nanocrystals. *J. Phys. Chem. B* 2004, *108* (17), 5250–5255. https://doi.org/10.1021/jp037699q.
- (14) Schmitt-Rink, S.; Ell, C.; Haug, H. Many-Body Effects in the Absorption, Gain, and Luminescence Spectra of Semiconductor Quantum-Well Structures. *Phys. Rev. B* 1986, 33
 (2), 1183–1189. https://doi.org/10.1103/PhysRevB.33.1183.
- (15) Klingshirn, C.; Haug, H. Optical Properties of Highly Excited Direct Gap Semiconductors. *Phys. Rep.* **1981**, 70 (5), 315–398. https://doi.org/10.1016/0370-1573(81)90190-3.
- (16) Yeltik, A.; Delikanli, S.; Olutas, M.; Kelestemur, Y.; Guzelturk, B.; Demir, H. V. Experimental Determination of the Absorption Cross-Section and Molar Extinction Coefficient of Colloidal CdSe Nanoplatelets. J. Phys. Chem. C 2015, 119 (47), 26768–26775. https://doi.org/10.1021/acs.jpcc.5b09275.
- (17) Ithurria, S.; Tessier, M. D.; Mahler, B.; Lobo, R. P. S. M.; Dubertret, B.; Efros, A. L. Colloidal Nanoplatelets with Two-Dimensional Electronic Structure. *Nat. Mater.* 2011, *10* (12), 936–941. https://doi.org/10.1038/nmat3145.

- (18) Brumberg, A.; Harvey, S. M.; Philbin, J. P.; Diroll, B. T.; Lee, B.; Crooker, S. A.; Wasielewski, M. R.; Rabani, E.; Schaller, R. D. Determination of the In-Plane Exciton Radius in 2D CdSe Nanoplatelets via Magneto-Optical Spectroscopy. ACS Nano 2019, 13 (8), 8589–8596. https://doi.org/10.1021/acsnano.9b02008.
- (19) Scott, R.; Achtstein, A. W.; Prudnikau, A. V.; Antanovich, A.; Siebbeles, L. D. A.; Artemyev, M.; Woggon, U. Time-Resolved Stark Spectroscopy in CdSe Nanoplatelets: Exciton Binding Energy, Polarizability, and Field-Dependent Radiative Rates. *Nano Lett.* 2016, 16 (10), 6576–6583. https://doi.org/10.1021/acs.nanolett.6b03244.
- (20) Shin, A. J.; Hossain, A. A.; Tenney, S. M.; Tan, X.; Tan, L. A.; Foley, J. J.; Atallah, T. L.; Caram, J. R. Dielectric Screening Modulates Semiconductor Nanoplatelet Excitons. *J. Phys. Chem. Lett.* **2021**, 4958–4964. https://doi.org/10.1021/acs.jpclett.1c00624.
- (21) Rowland, C. E.; Fedin, I.; Diroll, B. T.; Liu, Y.; Talapin, D. V.; Schaller, R. D. Elevated Temperature Photophysical Properties and Morphological Stability of CdSe and CdSe/CdS Nanoplatelets. *J. Phys. Chem. Lett.* 2018, 9 (2), 286–293. https://doi.org/10.1021/acs.jpclett.7b02793.
- (22) Geiregat, P.; Tomar, R.; Chen, K.; Singh, S.; Hodgkiss, J. M.; Hens, Z. Thermodynamic Equilibrium between Excitons and Excitonic Molecules Dictates Optical Gain in Colloidal CdSe Quantum Wells. *J. Phys. Chem. Lett.* **2019**, *10*, 3637–3644. https://doi.org/10.1021/acs.jpclett.9b01607.
- (23) Homburg, O.; Michler, P.; Heinecke, R.; Gutowski, J.; Wenisch, H.; Behringer, M.; Hommel, D. Biexcitonic Gain Characteristics in ZnSe-Based Lasers with Binary Wells. *Phys. Rev. B* **1999**, *60* (8), 5743–5750. https://doi.org/10.1103/PhysRevB.60.5743.
- (24) Kreller, F.; Lowisch, M.; Puls, J.; Henneberger, F. Role of Biexcitons in the Stimulated

- Emission of Wide-Gap II-VI Quantum Wells. *Phys. Rev. Lett.* **1995**, *75* (12), 2420–2423. https://doi.org/10.1103/PhysRevLett.75.2420.
- (25) Ding, J.; Jeon, H.; Ishihara, T.; Hagerott, M.; Nurmikko, A. V.; Luo, H.; Samarth, N.; Furdyna, J. Excitonic Gain and Laser Emission in ZnSe-Based Quantum Wells. *Phys. Rev. Lett.* **1992**, *69* (11), 1707–1710. https://doi.org/10.1103/PhysRevLett.69.1707.
- (26) Shah, J.; Leheny, R. F.; Wiegmann, W. Low-Temperature Absorption Spectrum in GaAs in the Presence of Optical Pumping. *Phys. Rev. B* **1977**, *16* (4), 1577–1580. https://doi.org/10.1103/PhysRevB.16.1577.
- Gibbs, H. M.; Gossard, A. C.; McCall, S. L.; Passner, A.; Wiegmann, W.; Venkatesan, T.
 N. C. Saturation of the Free Exciton Resonance in GaAs. *Solid State Commun.* 1979, 30 (5), 271–275. https://doi.org/10.1016/0038-1098(79)90075-9.
- (28) Bohnert, K.; Schmieder, G.; Klingshirn, C. Gain and Reflection Spectroscopy and the Present Understanding of the Electron–Hole Plasma in II–VI Compounds. *Phys. Status Solidi* **1980**, *98* (1), 175–188. https://doi.org/10.1002/pssb.2220980117.
- (29) Skettrup, T. Experimental Evidence for Electron-Hole Liquid in ZnO. *Solid State Commun.* 1977, 23 (10), 741–744. https://doi.org/10.1016/0038-1098(77)90484-7.
- (30) Chernikov, A.; Ruppert, C.; Hill, H. M.; Rigosi, A. F.; Heinz, T. F. Population Inversion and Giant Bandgap Renormalization in Atomically Thin WS 2 Layers. *Nat. Photonics* **2015**, 9 (7), 466–470. https://doi.org/10.1038/nphoton.2015.104.
- (31) Li, Q.; Lian, T. Area- and Thickness-Dependent Biexciton Auger Recombination in Colloidal CdSe Nanoplatelets: Breaking the "Universal Volume Scaling Law." *Nano Lett.* 2017, 17 (5), 3152–3158. https://doi.org/10.1021/acs.nanolett.7b00587.
- (32) Li, Q.; Liu, Q.; Schaller, R. D.; Lian, T. Reducing the Optical Gain Threshold in Two-

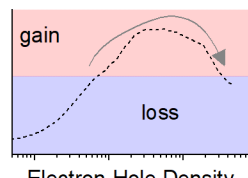
- Dimensional CdSe Nanoplatelets by the Giant Oscillator Strength Transition Effect. *J. Phys. Chem. Lett.* **2019**, *10* (7), 1624–1632. https://doi.org/10.1021/acs.jpclett.9b00759.
- (33) Smirnov, A. M.; Zharkova, E. V.; Golinskaya, A. D.; Kozlova, M. V.; Saidzhonov, B. M.; Vasiliev, R. B.; Dneprovskii, V. S. Saturable Absorption of CdSe/CdS Nanoplatelets Colloidal Solution (Conference Presentation). In *Nonlinear Optics and Applications XI*; Bertolotti, M., Zheltikov, A. M., Eds.; SPIE, 2019; p 14. https://doi.org/10.1117/12.2521047.
- (34) Zhang, Z.; Zhang, S.; Gushchina, I.; Guo, T.; Brennan, M. C.; Pavlovetc, I. M.; Grusenmeyer, T. A.; Kuno, M. Excitation Energy Dependence of Semiconductor Nanocrystal Emission Quantum Yields. J. Phys. Chem. Lett. 2021, 12 (16), 4024–4031. https://doi.org/10.1021/acs.jpclett.1c00811.
- (35) Tonti, D.; Van Mourik, F.; Chergui, M. On the Excitation Wavelength Dependence of the Luminescence Yield of Colloidal CdSe Quantum Dots. *Nano Lett.* **2004**, *4* (12), 2483–2487. https://doi.org/10.1021/nl0486057.
- (36) Hoheisel, W.; Colvin, V. L.; Johnson, C. S.; Alivisatos, A. P. Threshold for Quasicontinuum Absorption and Reduced Luminescence Efficiency in CdSe Nanocrystals. *J. Chem. Phys.* **1994**, *101* (10), 8455–8460. https://doi.org/10.1063/1.468107.
- (37) Li, B.; Brosseau, P. J.; Strandell, D. P.; Mack, T. G.; Kambhampati, P. Photophysical Action Spectra of Emission from Semiconductor Nanocrystals Reveal Violations to the Vavilov Rule Behavior from Hot Carrier Effects. *J. Phys. Chem. C* 2019, 123 (8), 5092–5098. https://doi.org/10.1021/acs.jpcc.8b11218.
- (38) Mikhailovsky, A. A.; Malko, A. V.; Hollingsworth, J. A.; Bawendi, M. G.; Klimov, V. I. Multiparticle Interactions and Stimulated Emission in Chemically Synthesized Quantum

- Dots. Appl. Phys. Lett. **2002**, 80 (13), 2380–2382. https://doi.org/10.1063/1.1463704.
- Garcia-Santamaria, F.; Chen, Y.; Vela, J.; Schaller, R. D.; Hollingsworth, J. A.; Klimov, V.
 I. Suppressed Auger Recombination in "Giant" Nanocrystals Boosts Optical Gain
 Performance. Nano Lett. 2009, 9 (10), 3482–3488. https://doi.org/10.1021/nl901681d.
- Ekimov, A. I.; Kudryavtsev, I. A.; Efros, A. L.; Yazeva, T. V.; Hache, F.; Schanne-Klein, (40)M. C.; Rodina, A. V.; Ricard, D.; Flytzanis, C. Absorption and Intensity-Dependent Photoluminescence Measurements on CdSe Quantum Dots: Assignment of the First Electronic Transitions. J. Opt. Soc. Am. В 1993. 10 (1),100. https://doi.org/10.1364/JOSAB.10.000100.
- (41) Miller, D. A. B. Optical Physics of Quantum Wells. In *Quantum Dynamics of Simple Systems*; Oppo G.-L., Barnett, S. M., Riis, E., Wilkinson, M., Eds.; Institute of Physics: London, 1996; pp 239–266.
- (42) Wu, W.; He, F.; Wang, Y. Reversible Ultrafast Melting in Bulk CdSe. J. Appl. Phys. 2016, 119 (5), 055701. https://doi.org/10.1063/1.4941019.
- (43) Goldstein, A. N.; Echer, C. M.; Alivisatos, A. P. Melting in Semiconductor Nanocrystals. *Science* **1992**, *256* (5062), 1425–1427. https://doi.org/10.1126/science.256.5062.1425.
- (44) Diroll, B. T.; Schaller, R. D. Heating and Cooling of Ligand-Coated Colloidal Nanocrystals in Solid Films and Solvent Matrices. *Nanoscale* 2019, 11 (17), 8204–8209. https://doi.org/10.1039/C9NR01473J.
- (45) Kirschner, M. S.; Hannah, D. C.; Diroll, B. T.; Zhang, X.; Wagner, M. J.; Hayes, D.; Chang,
 A. Y.; Rowland, C. E.; Lethiec, C. M.; Schatz, G. C.; Chen, L. X.; Schaller, R. D. Transient
 Melting and Recrystallization of Semiconductor Nanocrystals under Multiple ElectronHole Pair Excitation. Nano Lett. 2017, 17 (9), 5314–5320.

- https://doi.org/10.1021/acs.nanolett.7b01705.
- (46) Diroll, B. T.; Guo, P.; Schaller, R. D. Heat Transfer at Hybrid Interfaces: Interfacial Ligand-to-Nanocrystal Heating Monitored with Infrared Pump, Electronic Probe Spectroscopy. *Nano Lett.* **2018**, *18* (12), 7863–7869. https://doi.org/10.1021/acs.nanolett.8b03640.
- (47) Guzelturk, B.; Utterback, J. K.; Coropceanu, I.; Kamysbayev, V.; Janke, E. M.; Zajac, M.; Yazdani, N.; Cotts, B. L.; Park, S.; Sood, A.; Lin, M. F.; Reid, A. H.; Kozina, M. E.; Shen, X.; Weathersby, S. P.; Wood, V.; Salleo, A.; Wang, X.; Talapin, D. V.; Ginsberg, N. S.; Lindenberg, A. M. Nonequilibrium Thermodynamics of Colloidal Gold Nanocrystals Monitored by Ultrafast Electron Diffraction and Optical Scattering Microscopy. ACS Nano 2020, 14 (4), 4792–4804. https://doi.org/10.1021/acsnano.0c00673.
- (48) Brumberg, A.; Kirschner, M. S.; Diroll, B. T.; Williams, K. R.; Flanders, N. C.; Harvey, S. M.; Leonard, A. A.; Watkins, N. E.; Liu, C.; Kinigstein, E. D.; Yu, J.; Evans, A. M.; Liu, Y.; Cuthriell, S. A.; Panuganti, S.; Dichtel, W. R.; Kanatzidis, M. G.; Wasielewski, M. R.; Zhang, X.; Chen, L. X.; Schaller, R. D. Anisotropic Transient Disordering of Colloidal, Two-Dimensional CdSe Nanoplatelets upon Optical Excitation. *Nano Lett.* 2021. https://doi.org/10.1021/acs.nanolett.0c03958.
- (49) Diroll, B. T.; Brumberg, A.; Leonard, A. A.; Panuganti, S.; Watkins, N. E.; Cuthriell, S. A.; Harvey, S. M.; Kinigstein, E. D.; Yu, J.; Zhang, X.; Kanatzidis, M. G.; Wasielewski, M. R.; Chen, L. X.; Schaller, R. D. Photothermal Behaviour of Titanium Nitride Nanoparticles Evaluated by Transient X-Ray Diffraction. *Nanoscale* 2021, 13 (4). https://doi.org/10.1039/d0nr08202c.
- (50) Kirschner, M. S.; Diroll, B. T.; Guo, P.; Harvey, S. M.; Helweh, W.; Flanders, N. C.; Brumberg, A.; Watkins, N. E.; Leonard, A. A.; Evans, A. M.; Wasielewski, M. R.; Dichtel,

- W. R.; Zhang, X.; Chen, L. X.; Schaller, R. D. Photoinduced, Reversible Phase Transitions Perovskite in All-Inorganic Nanocrystals. Nat. Commun. 2019, **(1)**. https://doi.org/10.1038/s41467-019-08362-3.
- Achermann, M.; Bartko, A. P.; Hollingsworth, J. A.; Klimov, V. I. The Effect of Auger (51)Heating on Intraband Carrier Relaxation in Semiconductor Quantum Rods. Nat. Phys. 2006, 2 (8), 557–561. https://doi.org/10.1038/nphys363.
- Pelton, M.; Ithurria, S.; Schaller, R. D.; Dolzhnikov, D. S.; Talapin, D. V. Carrier Cooling Colloidal Quantum Wells. Nano Lett. 2012, 6158-6163. in 12 (12),https://doi.org/10.1021/nl302986y.

SYNOPSIS



Electron-Hole Density